ORIGINAL PAPER

Nature Friendly Single Atom Pt Catalyst For Propane Dehydrogenation

Saeed K. Amini*

*Chemistry and Chemical Engineering Research Center of Iran, Tehran, Iran

Received: 25 May 2025, Accepted: 2 August 2025

DOI: 10.22063/poj.2025.35707.1362

ABSTRACT

Activity of 111 surface of PtGa alloy in which three atom Pt centers are covered by In atoms is investigated as single atom Pt catalyst of propane dehydrogenation (PDH) by using quantum mechanical (QM) calculations. Periodic density functional theory (DFT) is applied in these calculations, utilizing PBE exchange-correlation functional with plane wave basis set of 680eV kinetic energy cut off. Calculated results give adsorption and conversion energies of propane to propylene including adsorption energies of intermediate states. Adsorption energies span is from -6 kJ/mole for propane up to -500 kJ/mole for $CH_3CH_2CH_2$ radical. Catalyzed propane to propylene's conversion energy is about -135 kJ/mole in comparison to about 150 kJ/mole of gas phase. Moderate adsorption energy value of about -120 kJ/mole for propylene and its higher conversion energy value of about 160 kJ/mole to $CH_3CH^*CH_2$ intermediate guarantee propylene slectivity and break of conversion chain after its formation. Lower activation energy values of first and second C—H breaks show that PDH reaction on this prposed catalyst is much faster than previously reported one in which three atom Pt centers were covered by toxic Pb atoms.

Keyword: PDH; Single atom Catalyst; PtGa/In; QM; plane Wave.

INTRODUCTION

As the second important produced feedstock of petrochemical industries next to ethylene, propylene is the main precursor in production of many of chemical materials that are used in industrial and domestic units. Importance of its production is so high that despite economic emergence due to coronavirus pandemic in 2020, its production rate passed 116 million tons. As its industrial production was started from 70 years ago, this high level of production rate is due to its different consumption types for many years. Bell et al. report its weigh percent production rate from different methods in 2016 and predicted demand up to 2021 (Supporting Figures 1 and 2, respectively) [1]. These figures show that an increasing gap was formed between its demand and supply values from 2007 [1]. They also show that about 80 percent of consumed propylene in around the world is byproduct of catalysis and steam cracking industrial units which are

designated for ethylene production [1]. Because rising rate of its demand is more than that of ethylene, use of other propylene production methods is inevitable. According to these figures, two most selective methods for propane production by more than 50% selectivity towards propylene are propane dehydrogenation (PDH) and advance methane to olefin (MTO) processes [1].

Selectivity of PDH towards propylene exceeds 85% that makes it the highest weight percent yield method of propylene production [1]. This reaction is possible via oxidative and non-oxidative processes [2]. Non-oxidative process which employs heterogeneous catalysts is exploited more than oxidative process because oxidative process suffers from less selectivity toward propylene production. Selectivity and stability of catalysts of non-oxidative process are determined via balancing between desorption of produced propylene and its involvement in undesirable side reactions such as cracking of next C–H(C) bonds and following coke production. In the Pt based catalysts, the Pt-Pt ensambles are known as active sites for undesirable dehydrogenation of propylene and its hydrogencraft. Thus, isolation of Pt atoms from each other on the catalyst's surface is an efficient method for inhibition from these undesirable side reactions. To this end, some novel studies report use of single atom like Pt catalysts for PDH in which Pt-Pt ensambles are absent [3-17]. Concurrently, many other single atom catalysts have been reported for this reaction [17-27].

Nakaya et al. tried to improve selectivity of PtGa alloy catalyst by covering its undesirable multi platinium centers via deposition of some mettalic atoms [14]. They isolated the Pt atoms of silica-supported PtGa catalyst from each other by Pb deposition. By using different Pt/Pb weight ratios, they produced a catalyst including isolated single Pt atoms which was nominated as single atom Pt catalyst [14]. It was stable for at least 96 hours in 600 ℃ with 96.6% of selectivity towards propylene and 30% of propane conversion. By using just one Pt/In weight ratio, they stated that use of indium instead of lead did not lead to more favorable results [14]. They state this conclusion in circumstances that despite extensive studies on different Pb covered catalysts, they reported just one study on In covered catalyst with Pt to In weight ratio of 2 and without any computational effort [14]. Intrestingly and according to Peer Review File of that article, reviewers didnot ask for any more explanation about In covered catalyst [14]. These evidences show that use of other Pt/In weight ratios may result in more favorable In covered PtGa catalyst than those of Pb covered one.

Meanwhile, these atoms' isolations in laboratory and experimental conditions are so hard jobs that limit more surveys about these situations and improvement of their precisions. To this end, reported experimental data are very limited in these cases and one do not have so much experimental data for comparison. Computational methods of chemistry have been employed in many PDH studies, specially from 2020, because of ommition of many high price and time consuming experimental asessments of proposed

catalysts [14-16, 18, 28-52]. Because these methods can easily model the isolated single atom catalysts, most of new PDH surveys benefit from computational methods alongside their experimental analyses to investigate and improve activity of catalysts [7-21, 51-58].

By considering mentioned drawbacks of Nakaya et al.'s study about In covered PtGa catalyst and efficiencies of computational chemistry methods, it encourages to investigate computationally this catalyst [14]. High value findings of this study will remove problems of the use of Pb and introduce a less hazardous catalyst [14]. Approval of this catalyst by computational method are followd by the search of PDH reaction mechanisem on it by comparing obtained reaction variables with that of four most accepted Langmuire-Hinshelwood mechanisms [49].

EXPERIMENTAL

Computational Details

It was tried to follow Nakaya et al.'s computational strategy in this study because the aim of this research was the survey of PDH on single atom PtGa/In catalyst by comparison of its charactristics and activity with that of PtGa/Pb [14]. To this end, the 111 surface of a cluster of PtGa crystal, covered with In atoms, was primarily used as input structure which includes 100 atoms (Figure 1) [59]. Crystal space group is first structural parameter that should be set in the beginig of a periodic quantum mechanical calculations. In spite of PtGa alloy that has given cubic $P2_13$ space group, addition of In atoms on its 111 surface changes its space group to triclinic *P1* [59]. Dimentions of central unit cell in periodic quantum mechanical calculations with this space group in the *x* and *y* directios were set to 12.18Å and 7.03Å, respectively. Dimention of *z* direction was set to 30Å in order to avoid interaction between adsorption slabs in this direction. All of three α, β and γ angles were set to 90^{o} according to triclinic *P1* space group. The three atom Pt centers in the *z* direction were inhibited from catalysis by covering each of them by an In atom. The single atom Pt centers were held uncovered in the *z* direction as adsorption and reaction centers that only one of them was used as adsorption and reaction center in iput file. Considering hexagonal structure of Pt centers on 111 surface of PtGa alloy, this arrangement inhibits interaction among adsorbed species with each other because remaining three single atom Pt centers of this central unit cell and their three images in neighboring unit cells surround this reaction center. They also can assist it, if adsorbates either move on the surface during geometry optimization or break to several parts that need extra adsorption centers.

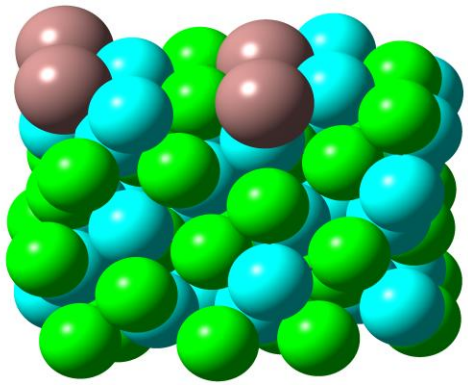

Figure 1. The 111 surface of PtGa crystal as single atom Pt catalyst in which three atom Pt centers are coverd by In atoms [59]. The blue, green and brown colors refer to Pt, Ga and In atoms, respectively.

The PBE exchange-correlation functional with plane wave basis set of 680*eV* kinetic energy cut off were applied as computational level of theory. Fermi dispersion index and convergence indexes of energy fluctuations, single electron orbital and ion position were set to 0.1*eV*, 1.0*10, $1.0*10^{-8}$ and $1.0*10^{-8}$, respectively. The cut off radius for interaction calculation by Ewald algorithm was set to 3Å. Because of hardware limitations and use of NWCHEM instead of Nakaya et al.'s use of CASTEP, it was not possible to set all the computational parameters as similar as each other [60, 61]. In order to apply Van der Waals interactions in NWCHEM, the vdw3 correction was applied.

Crystal symmetry of geometry optimized structures were distorted and different from input structures when dimentions of central unit cell were optimized in accordance with Nakaya et al.'s article. This is due to implementation of lowest level of symmetry for crystal structure that states a higher level of crystal symmetry should be inforced if it is possible. In order to apply a higher level of symmetry on crystal astructure, the applicable hexagonal $P6_5$ or $P6_3/mmc$ space groups were employed by special choice of atoms in the *x* and *y* directions. These space groups were selected because they are consistent with hexagonal structure of Pt centers. On the other hand, one can produce several similar slabs with large distances in *z* direction by setting its dimention to a large value and survey PDH reaction by seating propane on these layers. Dimentions of central unit cell in the *x*, *y* and *z* directions were set to 7.03, 7.03 and 100Å, respectively. The γ angle was set to 120. Because these space groups consider several layers in calculations instead of one layer of *P1* space group, computational time were increased so much that cause to calculations' corruption due to hrdware resource limitations. Thus, number of atomic layers of structure of Figure 1 were halved and number of atoms were decreased to 50 atoms from previous 100 atoms.

RESULTS AND DISCUSSION

Two main steps of a periodic quantum mechanical calculation are adjustment of *k*-point meshes and energy cut off values for accurate sampling of brilloin zone and precise determining of plane waves' energies, respectively. To this end, catalyst structure without adsorbed species was subject to geometry optimization with different *k*-point meshes and energy cut off values. Summarized results of these calculations in Table 1 show that due to use of big number of atoms in central unit cell, their changes have no significant effect on the energy of catalyst. Thus, 1×1×1 *k*-point mesh with 70*Ry* energy cut off values are obtained as optimized variables that may be used in subsequent calculations. Meanwhile, due to better proficiency reported for 3×3×3 *k*-point mesh in literatures, it was employed in subsequent calculations. As energy of catalyst was dectreased by increasing the energy cut off from 20 to 70*Ry*, it was concluded that cut off values larger than 70*Ry* are necessary to have convergence. Meanwhile, according to literatures, energy cut off values larger than 700*eV* cause to drastic errors in computational results and they are not recomended. On the other hand, due to very small difference between catalyst energies of calculations with 50 and 70*Ry* cut off values and considering very different spent computer time for these calculations, the 50*Ry* or 680*eV* was selected as optimized cut off value in subsequent calculations.

Table 1. Energies of optimized geometries of adsorbate free PtGa/In catalyst with different *k*-point mesh and energy cut off values.

Energy Cut Off (*Ry*)	*k*-point mesh	Energy of optimized geometry (*Hartree*)
20	1×1×1	-785.858256
20	3×3×3	-785.968263
30	3×3×3	-786.051143
40	3×3×3	-786.113021
45	3×3×3	-786.164236
50	3×3×3	-786.206193
55	3×3×3	-786.216573
60	3×3×3	-786.219742
70	3×3×3	-786.221856

By reaching to optimized values for *k*-point mesh and cut off value, propane, propylene and corresponding radicals and intermediates were deposited over catalyst to run subsequent quantum mechanical calculations by using these complexes of adsorbates and adsorbents. Most probable orientations of propane, propylene and their related counterparts, such as radicals and intermediate states, on the 111 surface of GaPt catalyst in which three Pt atom catalyst centers were covered by In atoms were constructed as input structures of geometry optimization calculations. Up and side views of these input structures are summarized in Figure 2. Out put geometries of these optimizations determine the resulting transition states' and products' structures, reaction rate and its mechanism. In order to obtain real optimized geometries that are free from any applied constraints on angles and bond lengths of adsorbed species, geometries of adsorbate-adsorbent complexes were optimized by fixing just two inferior Pt and two inferior Ga layers of catalyst. For example, in the activated $CH_3CH_2CH_2H^*$ and $CH_3CH^*HCH_2$ structures, in which C—H bonds of * recognized hydrogen atoms were elongated in input structure, were optimized without any constraint on activated bonds. Similar to optimized structures of adsorbate free catalyst, In atoms of geometry optimized structures of these complexes remain in their initial positions that supports catalyst persistence against distortion during geometry optimization. Figure 2 includes up and side views of resulting structures of geometry optimization calculations beside those of input structures. In the optimized structures of all species including CH_3CHCH_2 and $CH_3CH_2CH_3$ molecules, $CH_3CH_2CH_2H^*$, $CH_3CHH^*CH_2$ and $CH_3CH^*CH_2$ intermediates and $CH_3CH_2CH_2$ radical on the single atom Pt catalytic center, they remain adsorbed on the catalyst surface which reflect their efficient adsorption against addition of In atoms.

Input Geometry		Output Geometryof Geometry Optimization	
Top View	Side View	Top View	Side View
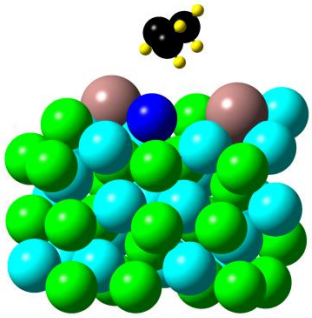	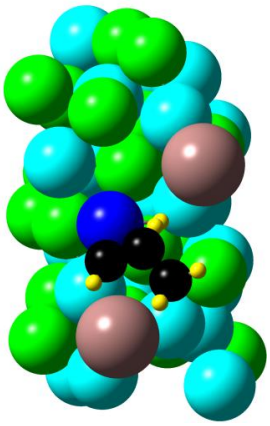	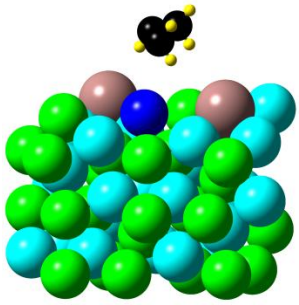	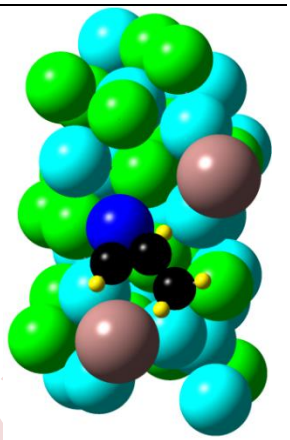
CH_3CHCH_2			
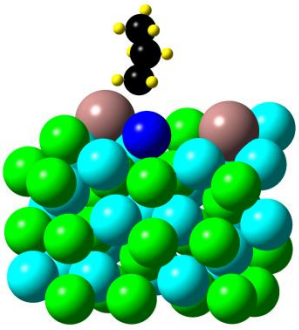	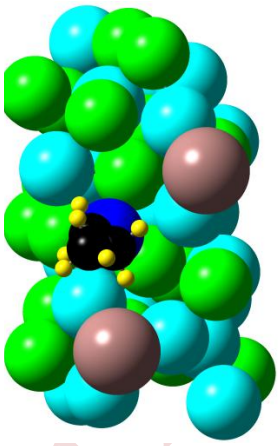	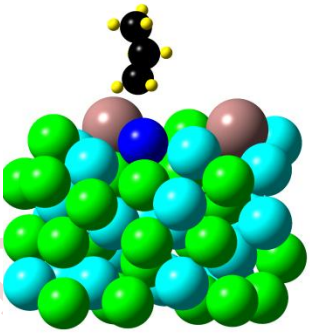	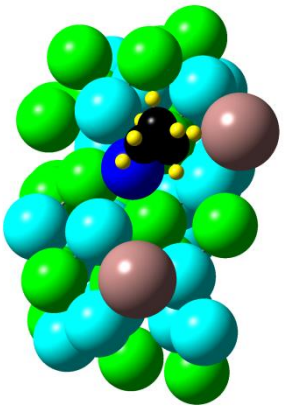
$CH_3CH_2CH_2$			
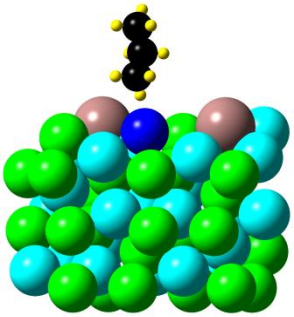	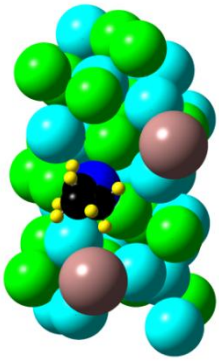	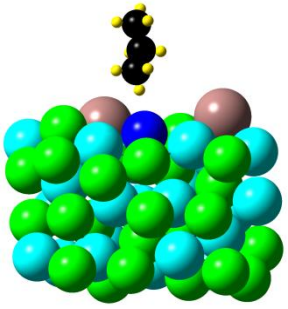	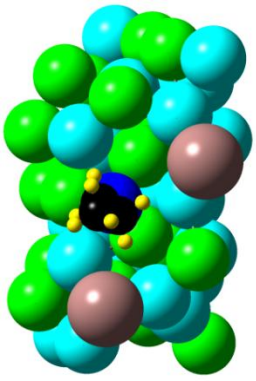
$CH_3CH_2CH_3$			

Input Geometry		Output Geometryof Geometry Optimization	
Top View	Side View	Top View	Side View
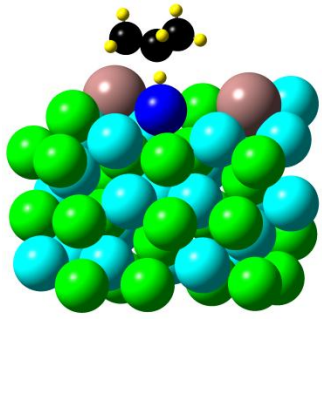	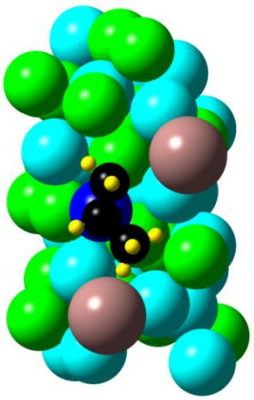	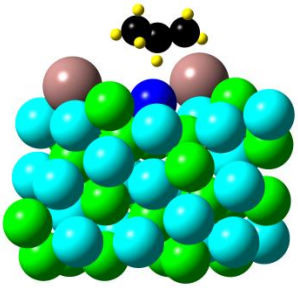	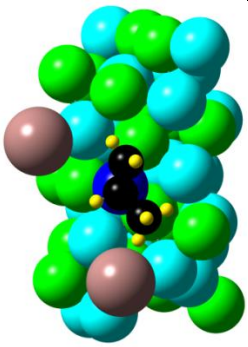
$CH_3CHH^*CH_2$			
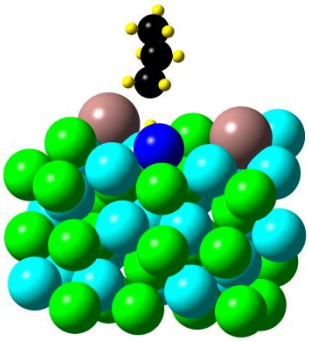	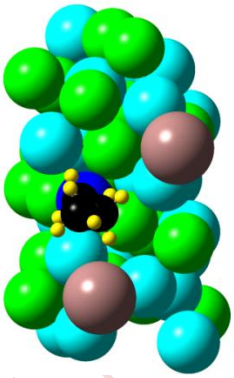	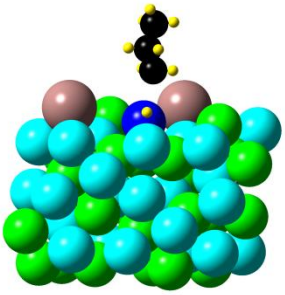	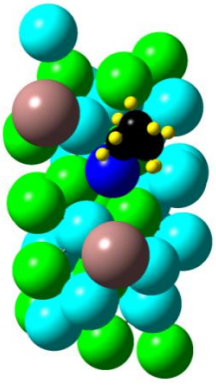
$CH_3CH_2CH_2H^*$			
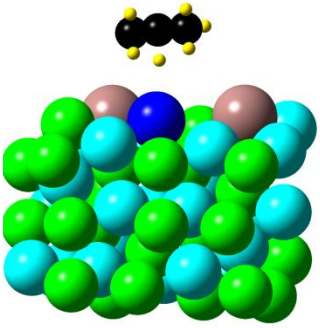	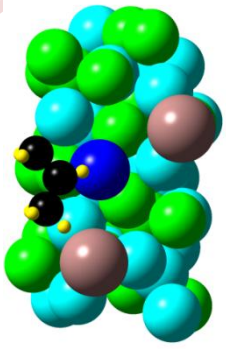	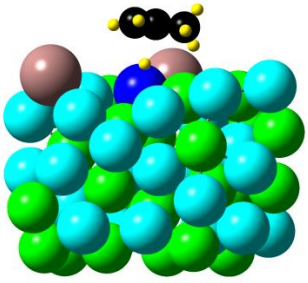	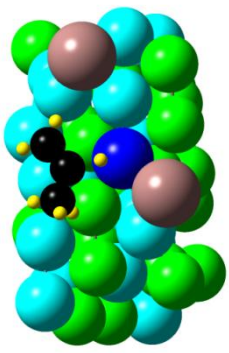
$CH_3CH^*CH_2$			

Figure 2- continued- Side and top views of input and geoemtry optimized output geometries of adsorbates on PtGa/In catalyst. The blue, dark blue, green and brown colors refer to Pt, single atom Pt center, Ga and In atoms, respectively.

In order to obtain energy changes in going from reactants to products, energy of catalyst of any complex without corresponding adsorbate and energy of any adsorbate of that complex without corresponding catalyst were calculated by using optimized geometries of corresponding adsorbates+catalyst complexes (left column of Figure 2). These energies along with total energies of corresponding complexes are summarized in Table 2 in Hartree/molecule because their conversion to kJ/mole makes very big digits. Of course, adsorption energies of adsorbates of corresponding complexes are summarized in this table in kJ/mole. This table shows that molecular adsorption of propylene on the single atom Pt center has moderate adsorption energy value of -118.06kJ/mole which is comparable with -108.3 kJ/mole of PtGa/Pb [14]. Significant difference between adsorption energies of molecular propane and propylene species reflects metal-*Π* interaction in the propylene which causes to higher adsorption energy value in this case. Very high adsorption energy values of 7H species of $CH_3CH_2CH_2$ radical and $CH_3CH^*HCH_2$ intermediate reflect existence of unpaired electron in these cases. This conclusion is certified by moderate adsorption energies of 6H and 8H intermediates of $CH_3CH_2CH_2H^*$ and $CH_3CH^*CH_2$ in which there are coupling between unpaired electrons of elongated H* atom and parental segment.

Table 2. Energies of catalyst of any structure without adsorbates and adsorbates of that structure without catalyst were calculated by using optimized geometries of adsorbates+catalyst structures. All in Hartree/species except to Adsorption of Output Structure values that are in kJ/mole.

Structure	Total	Catalyst	Output Structure	Adsorption of Output Structure
CH_3CHCH_2	-806.7797590	-786.175672	-20.64905496	-118.06
$CH_3CH_2CH_2$	-807.5839912	-786.177345	-21.21543835	-502.02
$CH_3CH_2CH_3$	-808.0680869	-786.191253	-21.87461240	-5.83
$CH_3CHH^*CH_2$	-807.5472561	-786.180426	-21.19424523	-453.12
$CH_3CH_2CH_2H^*$	-808.0737856	-786.189852	-21.86253412	-56.18
$CH_3CH^*CH_2$	-806.6185625	-786.184182	-20.40864523	-67.57

Conversion energies of reactants to products in kJ/mole which are obtained by using data of Table 2 are summarized in Table 3. These values that imply their energy differences over catalyst are obtained by subtracting the adsorption energy of each species and corresponding bare catalyst's energy from total energy of their complex. This table also includes gas phase calculations data for comparison. Despite gas phase calculation in which formation of propylene from propane is 147.6 kJ/mole endothermic, this reaction is exothermic on the catalyst surface in $CH_3CH_2CH_2H^*$ and $CH_3CH_2CH_3$ adsorption states by -98.9 and -

134.3 kJ/mole, respectively. Meanwhile, conversion of $CH_3CHH^*CH_2$ and $CH_3CH_2CH_2$ species to propylene on the catalyst are endothermic by 118.3 and 70.7 kJ/mole, respectively. On the other hand, adsorption energies of seven hydrogen species with unpaired electron are so high that their conversion to propylene by leaving an adsorbed radical H cannot compensate it.

Table 3. Conversion energies of reactants to products in kJ/mole.

Reactant	Product	Conversion Energy	Gas Phase
$CH_3CH_2CH_3$		-134.26	147.61
$CH_3CH_2CH_2H^*$		-98.87	
$CH_3CH_2CH_2$	CH_3CHCH_2	70.74	
$CH_3CHH^*CH_2$		118.29	
$CH_3CH_2CH_3$	$CH_3CH_2CH_2$	799.03	
$CH_3CH_2CH_2H^*$		834.42	
$CH_3CH_2CH_3$	$CH_3CHH^*CH_2$	653.69	
$CH_3CH_2CH_2H^*$		689.08	
$CH_3CH_2CH_3$	$CH_3CH_2CH_2H^*$	76.98	
CH_3CHCH_2	$CH_3CH^*CH_2$	118.15	

Reaction coordinate of PDH is summarized in Figure 3. Due to higher activation energies of first and second transition states in proposed In covered PtGa catalyst, it shows less activity relative to Pt single-atom, Pt_4 and Pt_3Sn single-cluster catalysts, all supported on g-C_3N_4 [55]. Due to very high adsorption energies of seven hydrogen species on this catalyst, their formation from eight hydrogen species are about 653-835 kJ/mole exothermic that release of their energies warranty supply of necessary energies for activation and conversion of $CH_3CH_2CH_3$ molecule to them and following cleavage of a hydrogen atom and propylene formation. This conclusion is certified by 77 kJ/mole released energy for propane conversion

to $CH_3CH_2CH_2H^*$ intermediate. On the other hand, it gives much higher activity relative to Pt dopped Cr2O3, PtGe, Pt/Cu, Pt_3Cu, Pt(111), Sn_1Pt, Pt1-S4/edge, Pt single atom of PtGa, Pt_3Sn single-cluster supported on Al_2O_3 and Pt3Sn(111) catalysts because of its very lower first and second transition states' energy barriers [10-15, 57]. These results are summarized in Figure 3.

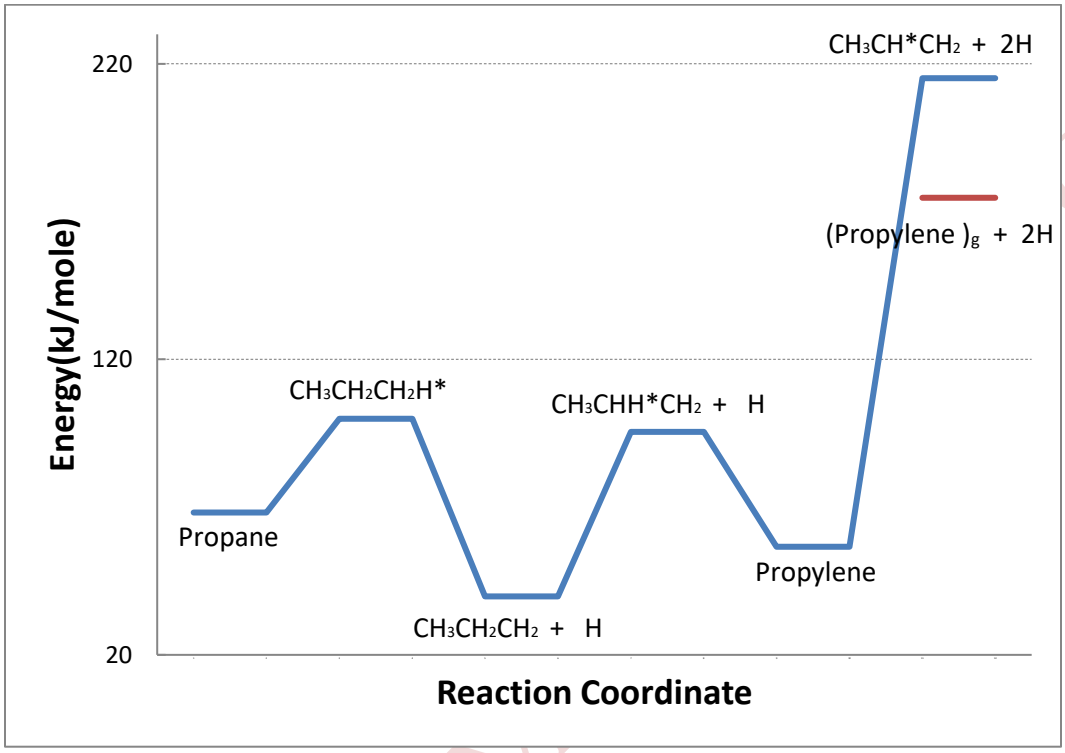

Figure 3. Energy diagram of PDH reaction. Hydrogen atoms recognized by asterisk have elongated bond lengths. All species are in adsorbed state except to recognized $(Propylene)_g$.

As table 2 shows, the moderate adsorption energy of molecular propylene on In covered PtGa is due to adsorption over single atom Pt center that shows lower tendency towards adsorption of molecular propylene in comparison to three atom Pt center. This moderate tendency towards propylene adsorption causes to higher selectivity of catalyst towards propylene via faster desorption of produced propylene in comparison to more proceed of reaction by propylene cracking (Figure 3). Thus it gives higher selectivity towards propylene relative to Pt single-atom, Pt_4 and Pt_3Sn single-cluster catalysts, all supported on g-C_3N_4, Pt_3Cu and Pt(111), due to faster desorption of propylene in comparison to its conversion to C_3H_5 [15, 55]. Of course, it gives lower selectivity towards propylene relative to Pt/Cu and Pt single atom of PtGa catalysts due to their higher activation energy towards C_3H_5 [14, 15].

These findings show that use of other Pt/In weight ratios results in higher activity of this catalyst relative to those of Pb which have not been reported by Nakaya et al. and corrects their data for precise In covered catalyst [14].

Reaction mechanism of PDH on this catalyst can be guessed by comparing calculated kinetics data with those of $PtSn_3$/K catalyst, calculated by Farjoo et al. for four most accepted Langmuire-Hinshelwood mechanisms [49, 62]. Considering the -118 kJ/mole adsorption energy of propylene, the reaction mechanism is more compatible with model 3 of $PtSn_3$/K catalyst in which this step is rate determining one (Supporting scheme 1) [62]. On the other hand, conversion energy of propane to propylene is obtained equal to -134 kJ/mole that is bigger than -71 kJ/mole of this model [62]. Thus, these calculations propose model 3 with higher rate constant than that of $PtSn_3$/K catalyst [62].

CONCLUSION

Calculated results show that reaction rate of PDH over PtGa catalyst in the presence of In is much faster than reported value in the presence of Pb [14]. These calclulations propose a single atom catalyst that beside its benefit from high selectivity of these sort of catalysts, has faster reaction rate and is free of toxic Pb element. Thus, it is recommended to repeat experiments in the presence of In in order to obtain more accurate results and survey this proposition.

REFERENCES

1. Bell AT, Alger MM, Flytzani-Stephanopoulos M, Gunnoe TB, Lercher JA, Stevens J, Alper J, Tran C (2016) The changing landscape of hydrocarbon feedstocks for chemical production: Implications for catalysis. In: National academies of sciences, engineering, and medicine, Washington, DC, USA
2. Otroshchenko T, Jiang G, Kondratenko VA, Rodemerck U, Kondratenko EV (2021) Current status and perspectives in oxidative, non-oxidative and CO2-mediated dehydrogenation of propane and isobutane over metal oxide catalysts. Chem Soc Rev 50: 473-527 [CrossRef]
3. Yang F, Zhang J, Chen J, Wang G, Yu T, Li Q, Shi Z, Sun Q, Zhuo R, Wang R (2024) Boosting propane dehydrogenation of defective S-1 stabilized single-atom Pt and ZnO catalysts via coordination environment regulation. Nano Res 17: 5884-5896 [CrossRef]
4. Nakaya Y, Furukawa S (2022) Tailoring single-atom platinum for selective and stable catalysts in propane dehydrogenation. ChemPlusChem 87: e202100560 [CrossRef]
5. Liu X, Wang X, Zhen S, Sun G, Pei C, Zhao Z, Gong J (2022) Support stabilized PtCu single-atom alloys for propane dehydrogenation. Chem Sci 13: 9537-9543 [CrossRef]

6. Yang Y, Liu Q, Wang J, Li P, Miao C, Liu J, Yang Y, Wang J, Wang X (2024) Hydroxy- or chlorine-anchored Pt single-atom in Al_2O_3: Which is better for propane dehydrogenation?. AIChE J 70: e18288 [CrossRef]
7. Dong C, Lai Z, Wang H (2023) Comprehensive mechanism and microkinetic model-driven rational screening of 3N-modulated single-atom catalysts for propane dehydrogenation. ACS Catal 13: 5529-5537 [CrossRef]
8. Zhao Q, Chen L, Ma S, Liu Z (2025) Data-driven discovery of Pt single atom embedded germanosilicate MFI zeolite catalysts for propane dehydrogenation. Nat Commun 16: 372 [CrossRef]
9. Lin J, Shen M, Zhang C, Bi S, Shen G, Gao F, Li W (2025) Active and stable platinum-indium single atom alloy catalysts for propane dehydrogenation. Chem Eng J 519 : 165243 [CrossRef]
10. Xing Y, Kang L, Ma J, Jiang Q, Su Y, Zhang S, Xu X, Li L, Wang A, Liu Z, Ma S, Liu XY, Zhang T (2023) Sn1Pt single-atom alloy evolved stable PtSn/nano-Al_2O_3 catalyst for propane dehydrogenation. Chinese J Catal 48: 164-174 [CrossRef]
11. Nakaya Y, Hayashida E, Asakura H, Takakusagi S, Yasumura S, Shimizu K, Furukawa S (2022) High-entropy intermetallics serve ultrastable single-atom Pt for propane dehydrogenation. J Am Chem Soc 144(35): 15944-15953 [CrossRef]
12. Dong C, Lai Z, Wang H (2024) Design of MoS_2 edge-anchored single-atom catalysts for propane dehydrogenation driven by DFT and microkinetic modeling. Phys Chem Chem Phys 26: 5303-5310 [CrossRef]
13. Jin D, Xu H, Zhu J, Cheng D (2023) Activation of Cr2O3 for propane dehydrogenation by doping with Pt single-atom promotor. Mol Catal 551: 113624 [CrossRef]
14. Nakaya Y, Hirayama J, Yamazoe S, Shimizu K, Furukawa S (2020) Single-atom Pt in intermetallics as an ultrastable and selective catalyst for propane dehydrogenation. Nat Commun 11: 2838 [CrossRef]
15. Sun G, Zhao Z, Mu R, Zha S, Li L, Chen S, Zang K, Luo J, Li Z, Purdy SC, Kropf AJ, Miller JT, Zeng L, Gong J (2018) Breaking the scaling relationship via thermally stable Pt/Cu single atom alloys for catalytic dehydrogenation. Nat Commun 9: 4454 [CrossRef]
16. Marcinkowski MD, Darby MT, Liu J, Wimble JM, Lucci FR, Lee S, Michaelides A, Flytzani-Stephanopoulos M, Stamatakis M, Sykes ECH (2018) Pt/Cu single-atom alloys as coke-resistant catalysts for efficient C–H activation. Nat Chem 10: 325-332 [CrossRef]
17. Xiong C, Dai S, Wu Z, Jiang D (2022) Single atoms anchored in hexagonal boron nitride for propane dehydrogenation from first principles. ChemCatChem 9/2022). ChemCatChem 14: e202200465 [CrossRef]
18. Chang QY, Wang KQ, Sui ZJ, Zhou XG, Chen D, Yuan WK, Zhu YA (2021) Rational design of single-atom-doped Ga_2O_3 catalysts for propane dehydrogenation: Breaking through volcano plot by Lewis acid-base interactions. ACS Catal 11: 5135-5147 [CrossRef]
19. Zhang W, Guo J, Ma H, Wen J, He C (2022) Anchoring of transition metals to CN as efficient single-atom catalysts for propane dehydrogenation. Chem Phys Lett 809: 140154 [CrossRef]
20. Qu Z, He G, Zhang T, Fan Y, Guo Y, Hu M, Xu J, Ma Y, Zhang J, Fan W, Sun Q, Mei D, Yu J (2024) Tricoordinated single-atom cobalt in zeolite boosting propane dehydrogenation. J Am Chem Soc 146: 8939-8948 [CrossRef]

21. Zhang Y, Shi S, Wang Z, Lan H, Liu L, Sun Q, Guo G, He X, Ji H (2024) Propane dehydrogenation on Ir single-atom catalyst modified by atomically dispersed Sn promoters in silicalite-1 zeolite. AIChE J 70: e18431 [CrossRef]
22. Zhang Q, Jiang X, Su Y, Zhao Y, Qiao B (2024) Catalytic propane dehydrogenation by anatase supported Ni single-atom catalysts. Chinese J Catal 57: 105-113 [CrossRef]
23. Ma R, Dean DP, Gao J, Wang M, Liu Y, Liang K, Wang J, Miller JT, Zhou B, Zou G, Kou J (2024) Lattice-embedded Ni single-atom catalyst on porous Al_2O_3 nanosheets derived from Ni-doped carbon dots for efficient propane dehydrogenation. Appl Catal B- Environ Energy 347: 123798 [CrossRef]
24. Guo L, Shi D, Zhang T, Ma Y, Qi G, Xu J, Sun Q (2025) Unsaturated cobalt single-atoms stabilized by silanol nests of zeolites for efficient propane dehydrogenation. Chinese J Catal 72: 323-333 [CrossRef]
25. Kang L, Zhu B, Gu Q, Duan X, Ying L, Qi G, Xu J, Li L, Su Y, Xing Y, Wang Y, Li G, Li R, Gao Y, Yang B, Liu XY, Wang A, Zhang T (2025) Light-driven propane dehydrogenation by a single-atom catalyst under near-ambient conditions. Nat Chem 17: 890-896 [CrossRef]
26. Chen J, Yue Y, Liu W (2025) Harnessing light for propane dehydrogenation: a single-atom catalyst milestone achieved under mild conditions. Sci China Chem 68: 2776-2778 [CrossRef]
27. Chernov AN, Sobolev VI, Gerasimov EY, Koltunov KY (2022) Propane dehydrogenation on Co-N-C/SiO_2 catalyst: The role of single-atom active sites. Catalysts 12: 1262 [CrossRef]
28. Cao L, Dai P, Zhu L, Yan L, Chen R, Liu D, Gu X, Li L, Xue Q, Zhao X (2020) Graphitic carbon nitride catalyzes selective oxidative dehydrogenation of propane. Appl Catal B- Environ 262: 118277 [CrossRef]
29. Huš M, Kopač D, Likozar B (2020) Kinetics of non-oxidative propane dehydrogenation on Cr_2O_3 and the nature of catalyst deactivation from first-principles simulations. J Catal 386: 126-138 [CrossRef]
30. Chen S, Pei C, Chang X, Zhao Z, Mu R, Xu Y, Gong J (2020) Coverage-dependent behaviors of vanadium oxides for chemical looping oxidative dehydrogenation. Angew Chem Int Ed 59: 22072-22079 [CrossRef]
31. Wang P, Senftle TP (2021) Theoretical insights into non-oxidative propane dehydrogenation over Fe3C. Phys Chem Chem Phys 23: 1401-1413 [CrossRef]
32. Wang T, Cui X, Winther KT, Abild-Pedersen F, Bligaard T, Nørskov JK (2021) Theory-aided discovery of metallic catalysts for selective propane dehydrogenation to propylene. ACS Catal 11: 6290-6297 [CrossRef]
33. Xie Z, Li Z, Tang P, Song Y, Zhao Z, Kong L, Fan X, Xiao X (2021) The effect of oxygen vacancies on the coordinatively unsaturated Al-O acid-base pairs for propane dehydrogenation. J Catal 397: 172-182 [CrossRef]
34. Liu J, Luo W, Yin Y, Fu X, Luo J (2021) Understanding the origin for propane non-oxidative dehydrogenation catalysed by d2-d8 transition metals. J Catal 396: 333-341 [CrossRef]
35. Sun X, Xue J, Ren Y, Li X, Zhou L, Li B, Zhao Z (2021) Revealing nature of active site and reaction mechanism of supported chromium oxide catalyst in propane direct dehydrogenation. Mol Catal 505: 111520 [CrossRef]
36. Sharma L, Jiang X, Wu Z, Baltrus J, Rangarajan S, Baltrusaitis J (2021) Elucidating the origin of selective dehydrogenation of propane on γ-alumina under H2S treatment and co-feed. J Catal 394: 142-156 [CrossRef]

37. Castro-Fernández P, Mance D, Liu C, Moroz IB, Abdala PM, Pidko EA, Copéret C, Fedorov A, Müller CR (2021) Propane dehydrogenation on Ga_2O_3-based catalysts: Contrasting performance with coordination environment and acidity of surface sites. ACS Catal 11: 907-924 [CrossRef]
38. Ye C, Peng M, Cui T, Tang X, Wang D, Jiao M, Miller JT, Li Y (2023) Revealing the surface atomic arrangement of noble metal alkane dehydrogenation catalysts by a stepwise reduction-oxidation approach. Nano Res 16: 4499-4505 [CrossRef]
39. Xiao L, Shan Y, Sui Z, Chen D, Zhou X, Yuan W, Zhu Y (2020) Beyond the reverse Horiuti–Polanyi mechanism in propane dehydrogenation over Pt catalysts. ACS Catal 10: 14887-14902 [CrossRef]
40. Araujo-Lopez E, Vandegehuchte BD, Curulla-Ferré D, Sharapa DI, Studt F (2020) Trends in the activation of light alkanes on transition-metal surfaces. J Phys Chem C 124: 27503-27510 [CrossRef]
41. Abdelgaid M, Dean J, Mpourmpakis G (2020) Improving alkane dehydrogenation activity on γ-Al2O3 through Ga doping. Catal Sci Technol 10: 7194-7202 [CrossRef]
42. Wang Z, Chen Y, Mao S, Wu K, Zhang K, Li Q, Wang Y (2020) Chemical insight into the structure and formation of coke on PtSn alloy during propane dehydrogenation. Adv Sustain Syst 4: 2000092 [CrossRef]
43. Fan X, Liu D, Sun X, Yu X, Li D, Yang Y, Liu H, Diao J, Xie Z, Kong L (2020) Mn-doping induced changes in Pt dispersion and PtxMny alloying extent on Pt/Mn-DMSN catalyst with enhanced propane dehydrogenation stability. J Catal 389: 450-460 [CrossRef]
44. Liu Z, Li Z, Li G, Wang Z, Lai C, Wang X, Pidko EA, Xiao C, Wang F, Li G (2020) Single-atom Pt+ derived from the laser dissociation of a platinum cluster: Insights into nonoxidative alkane conversion. J Phys Chem Lett 11: 5987-5991 [CrossRef]
45. Li A, Tian D, Zhao Z (2020) DFT studies on the reaction mechanism for the selective oxidative dehydrogenation of light alkanes by BN catalysts. New J Chem 44: 11584-11592 [CrossRef]
46. Chang Q, Wang K, Hu P, Sui Z, Zhou X, Chen D, Yuan W, Zhu Y (2020) Dual-function catalysis in propane dehydrogenation over Pt1-Ga2O3 catalyst: Insights from a microkinetic analysis. AIChE J 66: e16232 [CrossRef]
47. Aly M, Fornero EL, Leon-Garzon AR, Galvita VV, Saeys M (2020) Effect of boron promotion on coke formation during propane dehydrogenation over Pt/γ-Al_2O_3 catalysts. ACS Catal 10: 5208-5216 [CrossRef]
48. Purdy SC, Ghanekar P, Mitchell G, Kropf AJ, Zemlyanov DY, Ren Y, Ribeiro F, Delgass WN, Greeley J, Miller JT (2020) Origin of electronic modification of platinum in a Pt_3V alloy and its consequences for propane dehydrogenation catalysis. ACS Appl Energy Mater 3:1410-1422 [CrossRef]
49. Fogler H (1999) Elements of chemical reaction engineering, 3rd Ed. In.: Prentice Hall International, Inc, New Jersey.
50. Zhang T, Lang X, Dong A, Wan X, Gao S, Wang L, Wang L, Wang W (2020) Difference of oxidation mechanism between light C_3-C_4 alkane and alkene over mullite YMn_2O_5 oxides catalyst. ACS Catal 10: 7269-7282 [CrossRef]
51. Ma F, Chang QY, Yin Q, Sui ZJ, Zhou XG, Chen D, Zhu YA (2020) Rational screening of single-atom-doped ZnO catalysts for propane dehydrogenation from microkinetic analysis. Catal Sci Technol 10: 4938-4951 [CrossRef]

52. Zhang J, Zhou RJ, Chang QY, Sui JZ, Zhou XG, Chen D, Zhu YA (2021) Tailoring catalytic properties of V2O3 to propane dehydrogenation through single-atom doping: A DFT study. Catal Today 368: 46-57 [CrossRef]
53. Chen S, Chai Y, Chen Y, Wei F, Pan X, Lin J, Lin S (2024) Peripheral P doping in Zn1/NC single-atom catalyst to enhance propane dehydrogenation reaction. Chem Eng Sci 291: 119919 [CrossRef]
54. Wei F, Cao L, Ge B, Chen Y, Pan X, Chai Y, Jing R, Hu X, Wang X, Lin J, Lin S (2025) Regulating peripheral nitrogen dopants in single-atom catalysts to enhance propane dehydrogenation. Angew Chem 137: e202416912 [CrossRef]
55. Pan J, Strugovshchikov E, Salóm-Català A, Novell-Leruth G, Kaźmierczak K, Curulla-Ferré D, Carbó JJ, Godard C, Ricart JM (2025) Propane dehydrogenation on Pt single-atom and Pt_4 and Pt_3Sn single-cluster supported on g-C3N4: A theoretical study. J Phys Chem C 129: 2477-2487 [CrossRef]
56. Song W, Kang Y, Yang M, Li Z, Chen L, Zhao Z, Liu J (2022) Promoting propane dehydrogenation via strain engineering on iridium single-atom catalyst. Fuel 311: 122580 [CrossRef]
57. Sun S, Sun G, Pei C, Zhao Z, Gong J (2021) Origin of performances of Pt/Cu single-atom alloy catalysts for propane dehydrogenation. J Phys Chem C 125: 18708-18716 [CrossRef]
58. Hannagan RT, Giannakakis G, Réocreux R, Schumann J, Finzel J, Wang Y, Michaelides A, Deshlahra P, Christopher P, Flytzani-Stephanopoulos M, Stamatakis M, Sykes ECH (2021) First-principles design of a single-atom–alloy propane dehydrogenation catalyst. Science 372: 1444-1447 [CrossRef]
59. Bhargava M, Gadalla A, Schubert K (1975) Koexistente phasen vom FeSi-Typ in den mischungen Ni-Pd-Ga und Ni-Pt-Ga. J Less-Common Met 42: 69-76 [CrossRef]
60. Segall MD, Lindan PJD, Probert MJ, Pickard CJ, Hasnip PJ, Clark SJ, Payne MC (2002) First-principles simulation: ideas, illustrations and the CASTEP code. J Phys Condens Matter 14: 2717-2744 [CrossRef]
61. Valiev M, Bylaska EJ, Govind N, Kowalski K, Straatsma TP, Van Dam HJ, Wang D, Nieplocha J, Apra E, Windus TL, de Jong W (2010) NWChem: A comprehensive and scalable open-source solution for large scale molecular simulations. Comput Phys Commun 181: 1477-1489 [CrossRef]
62. Farjoo A, Khorasheh F, Niknaddaf S, Soltani M (2011) Kinetic modeling of side reactions in propane dehydrogenation over Pt - Sn/γ - Al2O3 catalyst. Sci Iran 18: 458-464 [CrossRef]